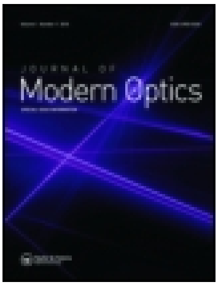

Journal of Modern Optics

Publication details, including instructions for authors and subscription information:
http://www.tandfonline.com/loi/tmop20

First-order analysis of a three-lens zoom system with the last lens fixed

Mau-Shiun Yeh [a] , Shin-Gwo Shiue [b] & Mao-Hong Lu [b]

[a] Chung Shan Institute of Science and Technology , PO Box 90008-8-10, Lung-Tan, Tao-Yuan, 325, Taiwan

[b] National Chiao Tung University, Institute of Electro-Optical Engineering , 1001 Ta Hsueh Road, Hsin Chu, 30050, Taiwan

Published online: 03 Jul 2009.

To cite this article: Mau-Shiun Yeh , Shin-Gwo Shiue & Mao-Hong Lu (1998) First-order analysis of a three-lens zoom system with the last lens fixed, Journal of Modern Optics, 45:2, 363-375, DOI: 10.1080/09500349808231695

To link to this article: http://dx.doi.org/10.1080/09500349808231695

JOURNAL OF MODERN OPTICS, 1998, VOL. 45, NO. 2, 363–375

First-order analysis of a three-lens zoom system with the last lens fixed

MAU-SHIUN YEH

Chung Shan Institute of Science and Technology, PO Box 90008-8-10, Lung-Tan, Tao-Yuan 325, Taiwan

SHIN-GWO SHIUE and MAO-HONG LU

National Chiao Tung University, Institute of Electro-Optical Engineering, 1001 Ta Hsueh Road, Hsin Chu 30050, Taiwan

(*Received 18 March 1997; revision received 3 July 1997*)

Abstract. A general analysis for the first-order solutions of three-lens zoom system with the last lens fixed is presented. The reasonable solution areas in the focal length diagrams are derived and shown graphically. The relation between the separation of the two front lenses and the image distance of middle lens in zooming is found to be a hyperbola. According to the different locations of centre of hyperbola, four cases are analysed. From the four hyperbolic graphs, we get six different types of zoom system. For each zoom type, we find the maximum range of focal length and the position where the maximum or minimum system length occurs during zooming.

1. Introduction

A zoom system is generally considered to consist of three parts: the focusing, zooming and fixed parts. The focusing part is placed in front of the zooming part, to adjust the object distance. The zooming part is literally used for zooming and the fixed rear part serves for controlling the focal length or magnification and reducing the aberrations of the whole system. Several of the published papers [1–4] concerning zoom have concentrated on the first-order zoom design. A two-optical-component method for designing zoom system has been proposed [2] and a three-lens zoom system with one lens fixed has been solved by this method. The three-lens system with the last lens fixed is widely used in many zooming systems, such as cameras, but the solution area has not been analysed so far.

In this paper, we use the grapho-analytical method [5] to solve the first-order layout of a three-lens zoom system with the last lens fixed. The possible solution areas in the focal length diagram are shown graphically. We find the relation between the separation of the two front lenses and the image distance of middle lens in zooming, which can be described by a hyperbola. We obtain four hyperbolae corresponding to the different positions of centre of the hyperbola. From the four hyperbolic graphs, we can get six types of zoom system and find the maximum variation range of focal length for each zoom type. The zoom position where the system has the maximum or minimum length is discussed.

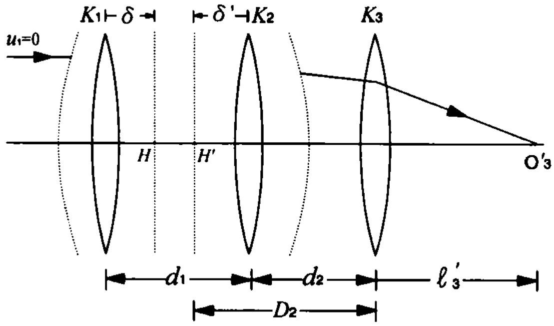

Figure 1. Gaussian diagram of three-lens zoom system with the third lens fixed. $\delta(\delta')$ is the distance from the first (second) lens to the first (second) principal plane H(H′) in the combined unit.

2. Theory

2.1. *Basic formulae*

In figure 1, an infinite-conjugate three-lens zoom system, with the last lens fixed and the others moving, has been analysed by the two-optical-component method [2], in which lenses 1 and 2 are combined as the first component and the last lens is regarded as the second component. The combined component has the focal length F_{12} and power K_{12}. d_1 and d_2 are the interlens separations between lenses 1 and 2 and between lenses 2 and 3 respectively. δ' is the distance from the second lens to the second principal plane H′ in the combined unit. K and F are the equivalent power and focal length respectively of the system. The related equations are then given by

$$K = K_{12} + K_3 - K_{12}K_3D_2, \tag{1}$$

$$\begin{aligned} D_2 &= d_2 - \delta' \\ &= d_2 + \frac{K_1}{K_{12}} d_1, \end{aligned} \tag{2}$$

$$K_{12} = K_1 + K_2 - K_1K_2d_1, \tag{3}$$

$$F = F_{12}M_3, \tag{4}$$

$$l'_3 = (1 - M_3)F_3, \tag{5}$$

where l'_3 and M_3 are the image distance and magnification of the F_3 lens.

Solving the above equations, from equations (1)–(4), we have

$$d_1 = F_1 + F_2 - \frac{F_1F_2}{F_{12}}, \tag{6}$$

$$d_2 = -\left(\frac{1}{M_3} - 1\right)F_3 + \left(1 - \frac{d_1}{F_1}\right)F_{12}. \tag{7}$$

Because the third lens is fixed during zooming, M_3 is constant. F is therefore proportional to F_{12}. In zooming, we change F and then obtain F_{12}, d_1 and d_2. From paraxial optics, we have

$$d_2 = l_2' - l_3 = (1 - M_2)F_2 - \left(\frac{1}{M_3} - 1\right)F_3. \tag{8}$$

Comparing equation (7) with equation (8), we find that

$$l_2' = \left(1 - \frac{d_1}{F_1}\right)F_{12}. \tag{9}$$

Substituting equation (6) into equation (9), we have

$$l_2' = \left(1 - \frac{F_{12}}{F_1}\right)F_2. \tag{10}$$

2.2. *Solution areas in the focal length diagram*

The interlens separations d_1 and d_2 must be positive in zooming. This gives some constraints on the solutions, that is on F_1, F_2 and F_3. Because the third lens is fixed, the image point of F_2 is also fixed during zooming. In this case, we can always find a lens F_3 to form a final real image from the lens equation and have a positive d_2, no matter where the image point of F_2 is. So we shall discuss only the solution areas under the constraint of positive d_1. From equation (6), we have

$$F_1 + F_2 - \frac{F_1F_2}{F_{12}} \geqslant 0. \tag{11}$$

According to the different signs of F_{12}, we have two cases as follows:

$$(F_1 - F_{12})(F_2 - F_{12}) - F_{12}^2 \leqslant 0 \qquad \text{if } F_{12} > 0 \tag{12}$$

and

$$(F_1 - F_{12})(F_2 - F_{12}) - F_{12}^2 \geqslant 0 \qquad \text{if } F_{12} < 0. \tag{13}$$

The curve for $(F_1 - F_{12})(F_2 - F_{12}) - F_{12}^2 = 0$ is a hyperbola with its centre at (F_{12}, F_{12}) in the F_1–F_2 coordinate graph. The solution distribution in the graph is thus divided into several areas by the hyperbolic curves. Each solution area has different solution ranges for F_{12} and d_1.

From the above analysis, we can illustrate the possible solution areas in the focal length diagrams according to the different combinations of F_1 and F_2, and the sign of F_{12}. Figure 2 shows the solution areas for $F_{12} > 0$ and $F_{12} < 0$ under the condition of positive d_1. The power signs of F_1 and F_2 in each area are shown in parentheses as (F_1, F_2). The sign of $F_1 + F_2$ is positive in the upper right section and negative in the lower left section. The solution ranges of F_{12} and d_1, and the related range of l_2' obtained from equation (10) for each solution area are shown in tables 1 and 2 with different signs of F_{12}. Using equation (10), we can show the sign of l_2' for each solution area in figure 3.

2.3. *Relation between the separation d_1 and the image distance of l_2'*

From equations (3) and (9), we have

$$[d_1 - (F_1 + F_2)](l_2' - F_2) - F_2^2 = 0 \tag{14}$$

or

able 1. Solution ranges of F_{12}, d_1 and l_2' for different solution areas under different combinations of lens types with positi

es of ses	Solution area	Range of F_{12}	Range of d_1	Range of l_2'	Used segment	Possible vertex hyperb
$F_2 > 0$ +)	(I) in figure 2(a)	$\frac{F_1F_2}{F_1+F_2} \leqslant F_{12} < \infty$	$0 \leqslant d_1 < F_1 + F_2$	$-\infty < l_2' \leqslant \frac{F_1F_2}{F_1+F_2}$	Segment 2a ($a_1 > 0$, $a_2 > 0$)	Positive tra axis (d_1 >
$F_2 > 0$ +)	(IIa) in figure 2(a)	$0 < F_{12} < \infty$	$F_1 + F_2 < d_1 < \infty$	$F_2 < l_2' < \infty$	Segment 1b ($a_1 > 0$, $a_2 > 0$)	Quadrant I
	(IIb) in figure 2(a)	$0 < F_{12} \leqslant \frac{F_1F_2}{F_1+F_2}$	$0 \leqslant d_1 < \infty$	$F_2 < l_2' \leqslant \frac{F_1F_2}{F_1+F_2}$	Segment 3 ($a_1 < 0$, $a_2 > 0$)	Quadrant I
$F_2 < 0$ -)	No solution	No solution	No solution	No solution	No solution	No solutio
$F_2 < 0$ -)	(IVa) in figure 2(a)	$0 < F_{12} < \infty$	$F_1 + F_2 < d_1 < \infty$	$F_2 < l_2' < \infty$	Segment 5 ($a_1 > 0$, $a_2 < 0$)	Positive tra axis (d_1 >
	(IVb) in figure 2(a)	$0 < F_{12} \leqslant \frac{F_1F_2}{F_1+F_2}$	$0 \leqslant d_1 < \infty$	$F_2 < l_2' \leqslant \frac{F_1F_2}{F_1+F_2}$	Segment 4a ($a_1 < 0$, $a_2 < 0$)	Positive tra axis (d_1 >

able 2. Solution ranges of F_{12}, d_1 and l_2' for different solution areas under different combinations of lens types with positi

s of es	Solution area	Range of F_{12}	Range of d_1	Range of l_2'	Used segment	Possible vertex hyperb
$F_2 > 0$ +)	(I) in figure 2(b)	$-\infty < F_{12} < 0$	$F_1 + F_2 < d_1 < \infty$	$F_2 < l_2' < \infty$	Segment 1a ($a_1 > 0$, $a_2 > 0$)	Quadrant
$F_2 > 0$ +)	(II) in figure 2(b)	$-\infty < F_{12} \leqslant \frac{F_1F_2}{F_1+F_2}$	$0 \leqslant d_1 < F_1 + F_2$	$-\infty < l_2' \leqslant \frac{F_1F_2}{F_1+F_2}$	Segment 2b ($a_1 > 0$, $a_2 > 0$)	Negative t axis (d_1
$F_2 < 0$ -)	(III) in figure 2(b)	$\frac{F_1F_2}{F_1+F_2} \leqslant F_{12} < 0$	$0 \leqslant d_1 < \infty$	$F_2 < l_2' \leqslant \frac{F_1F_2}{F_1+F_2}$	Segment 4b ($a_1 < 0$, $a_2 < 0$)	Negative t axis (d_1
$F_2 < 0$ -)	(IV) in figure 2(b)	$-\infty < F_{12} \leqslant \frac{F_1F_2}{F_1+F_2}$	$0 \leqslant d_1 < F_1 + F_2$	$-\infty < l_2' \leqslant \frac{F_1F_2}{F_1+F_2}$	Segment 6 ($a_1 > 0$, $a_2 < 0$)	Quadrant

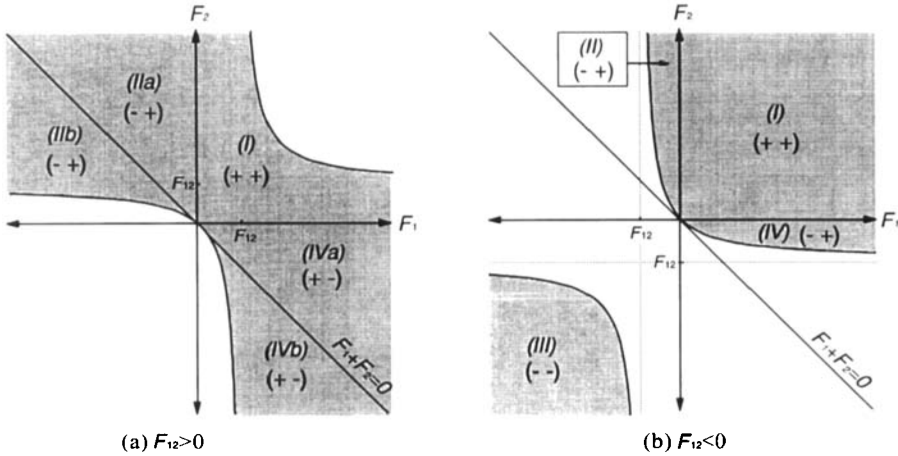

Figure 2. Solution areas (shaded) for different combinations of lens types under the condition of positive d_1: (a) $F_{12} > 0$; (b) $F_{12} < 0$.

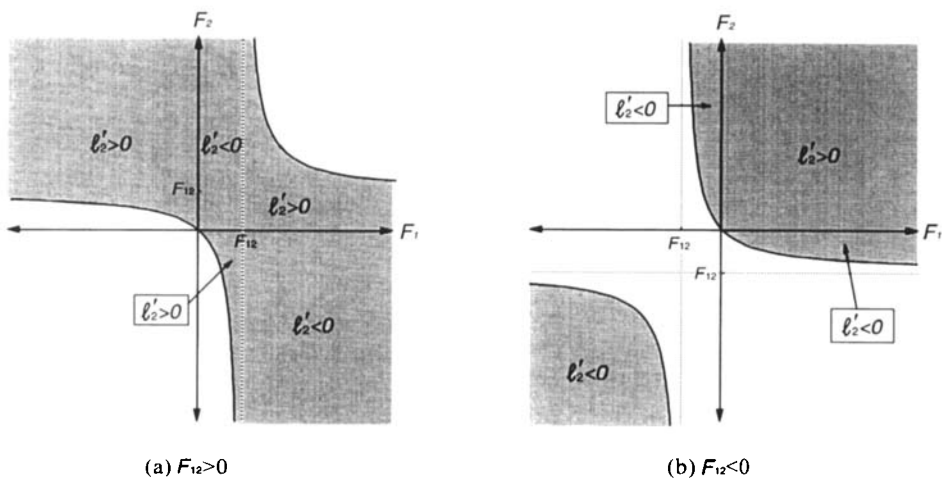

Figure 3. Sign distributions of l_2' in the solution areas: (a) $F_{12} > 0$; (b) $F_{12} < 0$.

$$(d_1 - a_1)(l_2' - a_2) = F_2^2, \tag{15}$$

where $a_1 = F_1 + F_2$ and $a_2 = F_2$.

The above equation describes a hyperbola with its centre at the coordinates (a_1, a_2) in the d_1–l_2' coordinate graph. Because the centre of the hyperbola can be located in one of the four quadrants depending on the signs of a_1 and a_2, we obtain four cases of hyperbolae shown in figures 4–7. The upper right hyperbolic curve has the vertex V_1 with $d_1 = a_1 + |F_2|$ and $l_2' = a_2 + |F_2|$ and the lower left hyperbolic curve has the vertex V_2 with $d_1 = a_1 - |F_2|$ an $l_2' = a_2 - |F_2|$. Because $a_2 = F_2$, one of the hyperbolic curves always intersects the transverse (d_1) axis at one vertex of hyperbola, that is V_1 or V_2. In figure 4, F_1 could be positive or negative. If $F_1 > 0$ (or $F_1 < 0$) is selected, the vertex V_2 is located on the positive transverse (or negative) axis. A similar situation occurs in figure 6.

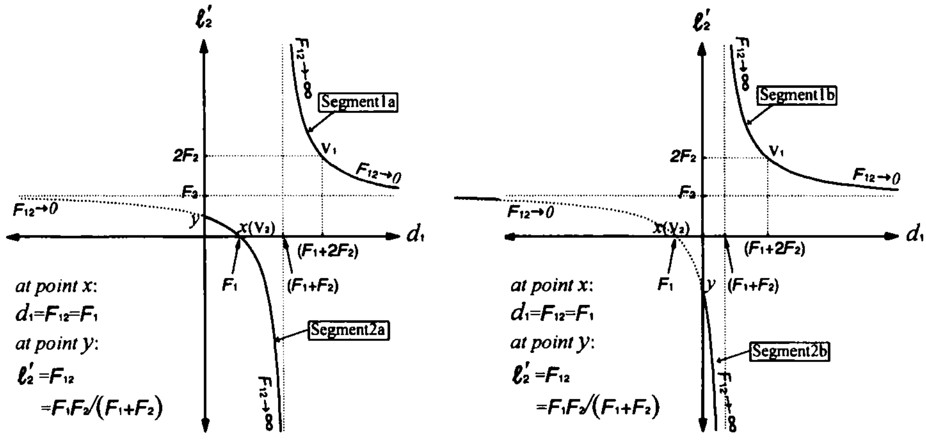

(a) $a_1>0$, $a_2>0$, and $F_1>0$ (b) $a_1>0$, $a_2>0$, and $F_1<0$

Figure 4. Hyperbola with its centre in the first quadrant of the d_1–l_2' coordinate diagram. V_1 and V_2 are the vertices of the hyperbola. The intersection coordinates of hyperbola and two axes are x and y respectively: (a) $F_1 > 0$; (b) $F_1 < 0$.

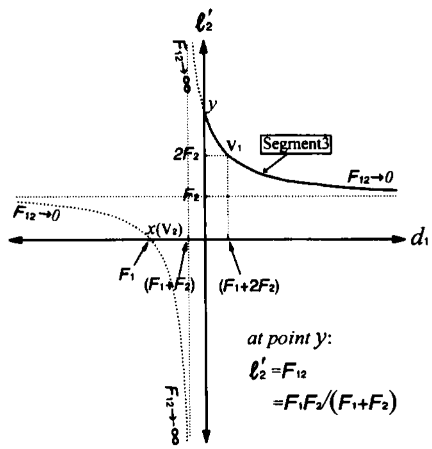

$a_1<0$ and $a_2>0$

Figure 5. Hyperbola with its centre in the second quadrant of the d_1–l_2' coordinate diagram.

From equations (6) and (10), we can solve the focal length F_{12} for each point on the hyperbola as follows:

$$F_{12} = \frac{F_1 F_2}{F_1 + F_2 - d_1} \tag{16}$$

or

$$F_{12} = \left(1 - \frac{l_2'}{F_2}\right) F_1. \tag{17}$$

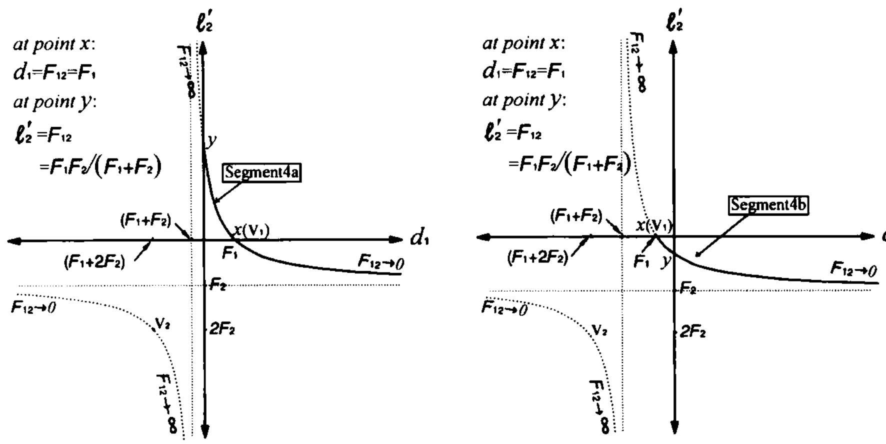

(a) $a_1<0$, $a_2<0$, and $F_1>0$ (b) $a_1<0$, $a_2<0$, and $F_1<0$

Figure 6. Hyperbola with its centre in the third quadrant of the d_1–l_2' coordinate diagram. (*a*) $F_1 > 0$; (*b*) $F_1 < 0$.

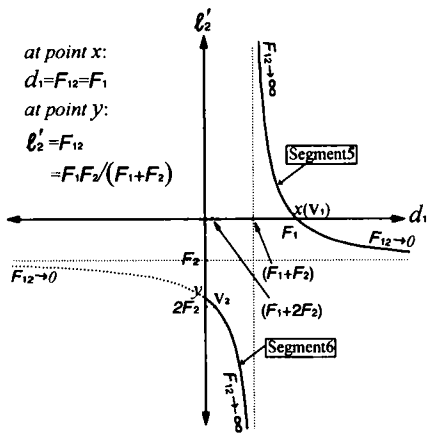

$a_1>0$ and $a_2<0$

Figure 7. Hyperbola with its centre in the fourth quadrant of the d_1–l_2' coordinate diagram.

In equation (16), if d_1 approaches infinity, F_{12} approaches zero. Similarly, if l_2' in equation (17) approaches infinity, F_{12} approaches infinity and the sign of F_{12} is determined by the sign of $-(F_1/F_2)l_2'$. Two cases for different signs of F_1/F_2 are obtained. If $F_1/F_2 < 0$, the values of F_{12} for the points on the upper-right and lower left hyperbolic curves are positive and negative respectively. On the other hand, if $F_1/F_2 > 0$, the values of F_{12} for the points on the upper right and lower left hyperbolic curves are negative and positive respectively.

In figure 4–7, the intersections of the hyperbola and the two axes are x and y corresponding to $l_2' = 0$ and $d_1 = 0$ respectively. As described before, x is the vertex V_1 or V_2. The value of F_{12} can be obtained from equation (17) by $l_2' = 0$. So we have

$$F_{12} = F_1. \tag{18}$$

Substituting equation (18) into equation (6), we get

$$d_1 = F_1. \tag{19}$$

Similarly, the values of F_{12} and l_2' at y obtained by $d_1 = 0$ in equations (16) and (17). We have

$$F_{12} = \frac{F_1 F_2}{F_1 + F_2} \tag{20}$$

$$l_2' = \frac{F_1 F_2}{F_1 + F_2}. \tag{21}$$

As mentioned before, a reasonable separation d_1 must be positive in zooming. So only the segments of hyperbola in the right-hand half of the d_1–l_2' coordinate graph are acceptable and shown as solid curves in figures 4–7. Six segments are found and labelled Segment followed by a number. Each segment represents the characteristics of a zoom system, including the constraints on a_1 and a_2 (or on F_1 and F_2) and the solution ranges of F_{12}, d_1 and l_2' in zooming. Therefore we can have six types of zoom system. In figures 4 and 6, the segment labels are followed by an extra letter a or b for two different combinations of F_1 and F_2.

The length of zoom system, which is the distance from lens 1 to image plane, is the sum of d_1, l_2', $-l_3$ and l_3'. The last two terms are constants because the third lens is fixed. From the property of a hyperbola, the value of $d_1 + l_2'$ has a minimum at the vertex V_1 with $d_1 = a_1 + |F_2|$ and $l_2' = a_2 + |F_2|$ for segments 1, 3, 4 and 5 and has a maximum at the vertex V_2 with $d_1 = a_1 - |F_2|$ and $l_2' = a_2 - |F_2|$ for segments 2 and 6. So the system length has an extreme value (maximum or minimum) at some position of zooming, that is not necessarily at one end of zooming, if the vertex of the hyperbolic curve is located in the right-hand half of the d_1–l_2' coordinate graph. In this case, the value of F_{12} is calculated as follows.

Substituting $d_1 = a_1 + |F_2|$ or $l_2' = a_2 + |F_2|$ into equation (16) or (17) for segments 1, 3, 4 and 5, we have

$$F_{12} = \begin{cases} -F_1 & \text{if } F_2 > 0, \quad (22) \\ F_1 & \text{if } F_2 < 0. \quad (23) \end{cases}$$

Similarly, substituting $D_1 = a_1 - |F_2|$ or $l_2' = a_2 - |F_2|$ into equation (16) or (17) for segments 2 and 6, we have

$$F_{12} = \begin{cases} F_1 & \text{if } F_2 > 0, \quad (24) \\ -F_1 & \text{if } F_2 < 0. \quad (25) \end{cases}$$

On the other hand, if the vertex of hyperbolic curve falls in the left-hand half of the d_1–l_2' coordinate graph, the maximum and minimum system lengths occur at the two ends of zooming.

2.4. *Related segment of hyperbola for different solution areas*

In section 2.2, we have analysed the reasonable solution areas in the focal length diagrams and their related solution ranges of F_{12}, d_1 and l_2'. From sections 2.2 and 2.3, we find that the ranges of F_{12}, d_1 and l_2' for each solution area shown in figure 2 and listed in tables 1 and 2 are always a part of hyperbola in one of the four

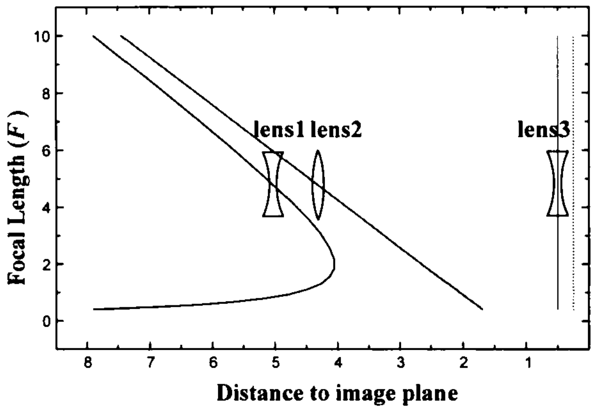

Figure 8. Loci of three-lens zoom system with $F_1 = -1$, $F_2 = 1{\cdot}2$, $F_3 = -0{\cdot}5$, $M_3 = 2$ and a zoom ratio of 25:1. The dotted line indicates the image position of middle lens. This system has $d_1 = 1{\cdot}4$, $l_2' = 2{\cdot}4$ and $F_{12} = 1$ at the position where the system length is minimum during zooming.

cases in figures 4–7, where d_1 is positive. The sixth and seventh columns in tables 1 and 2 show the constraints on the signs of a_1 and a_2, the used segment of hyperbola, and the possible vertex locations of related hyperbolic curve in the four quadrants for each solution area. The various quadrants are denoted (I), (II), (III) and (IV) respectively.

2.5. *Six types of zoom systems*

Figures 4–7 have shown that each of the six segments represents the characteristics of a zoom system. Six different types of zoom system are thus discussed as follows.

2.5.1. *Type I*

For segment 1 in figure 4, the range of F_{12} starts from plus or minus infinity to zero depending on the sign of F_1/F_2. From tables 1 and 2, we find that two solution areas with positive F_2 meet this type. Because the vertex of related hyperbolic curve falls in the first quadrant of the d_1–l_2' coordinate graph, the system length always passes through a minimum value during zooming. In this type, we choose the second solution area in table 1 as an example. According to the constraints on F_1 and F_2 in the solution area (IIa) in figure 2(*a*), we have $F_1 = -1$ and $F_2 = 1{\cdot}2$. Referring to the solution range of l_2', we have $F_3 = -0{\cdot}5$ and $M_3 = 2$ to keep d_2 positive during zooming. In theory, F_{12} can be from plus infinity to zero. here we choose the range of F_{12} from 5 to $0{\cdot}2$ with a zoom ratio of 25:1. The focal length range of system is from 10 to $0{\cdot}4$ given by equation (4). When the system length has the minimum value, we have $d_1 = 1{\cdot}4$, $l_2' = 2{\cdot}4$ and $F_{12} = 1$. The lens loci in zooming are shown in figure 8, with the focal length F as ordinate. the image position of the middle lens, that is the object position of the third lens, is fixed and shown as a dotted line.

2.5.2. *Type II*

For segment 2 in figure 4, the range of F_{12} is from plus or minus infinity to $F_1F_2/(F_1 + F_2)$. In tables 1 and 2, two solution areas with positive F_2 belong to

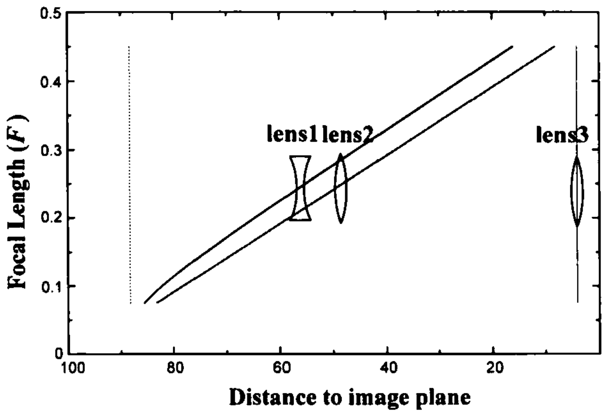

Figure 9. Loci of three-lens zoom system with $F_1 = -1$, $F_2 = 10$, $F_3 = 4$, $M_3 = -0{\cdot}05$, $l'_3 = 4{\cdot}2$ and a zoom of 6:1. The maximum and minimum system lengths occur at the two ends of zooming.

this type. the vertex of the related hyperbolic curve is located on the transverse axis. If the vertex is on the positive transverse axis, the system has a maximum length in zooming with $d_1 = F_1$, $l'_2 = 0$ and $F_{12} = F_1$. Here we choose the second solution area in table 2 as an example. According to the constraints on F_1 and F_2 in the solution area (II) in figure 2 (*b*) and the range of l'_2, we have $F_1 = -1$, $F_2 = 10$, $F_3 = 4$ and $M_3 = -0{\cdot}05$. We have the theoretical range of F_{12} from minus infinity to $-1{\cdot}111$. In this example, we choose F_{12} from -9 to $-1{\cdot}5$ with a zoom ratio of 6:1. The zoom loci are shown in figure 9.

2.5.3. *Type III*

For segment 3 in figure 5, the range of F_{12} is from $F_1F_2/(F_1F_2)$ to 0. Only the third solution area in table 1, with positive F_{12} and F_2, belongs to this type. In this case, the vertex of related hyperbolic curve can be located in the first or second quadrant. With the constraints on F_1 and F_2 in the solution area (IIb) in figure 2 (*a*) and the range of l'_2, we have $F_1 = -1$, $F_2 = 0{\cdot}95$, $F_3 = -2$ and $M_3 = 1{\cdot}5$. In theory, the maximum range of F_{12} is from 19 to 0. In this example, we choose F_{12} from 4 to $0{\cdot}25$. The system has a zoom ratio of 16:1 and has the minimum length with $d_1 = 0{\cdot}9$, $l'_2 = 1{\cdot}9$, and $F_{12} = 1$. The zoom loci are shown in figure 10.

2.5.4. *Type IV*

For segment 4 in figure 6, the range of F_{12} is from $F_1F_2/(F_1 + F_2)$ to 0. In tables 1 and 2, two solution areas with negative F_2 belong to this type. In this case, the vertex of the hyperbolic curve is located on the transverse axis. Here we use the sixth solution area in table 1 as an example. Using the solution area (IVb) in figure 2 (*a*) and the range of l'_2, we have $F_1 = 1$, $F_2 = -1{\cdot}2$, $F_3 = 2$ and $M_3 = -1$. We have the theoretical range of F_{12} from 6 to 0. In this example, we choose F_{12} from $1{\cdot}5$ to $0{\cdot}1$. The system has a zoom ratio of 15:1 and has the minimum length with $d_1 = 1$, $l'_2 = 0$ and $F_{12} = 1$. The zoom loci are shown in figure 11.

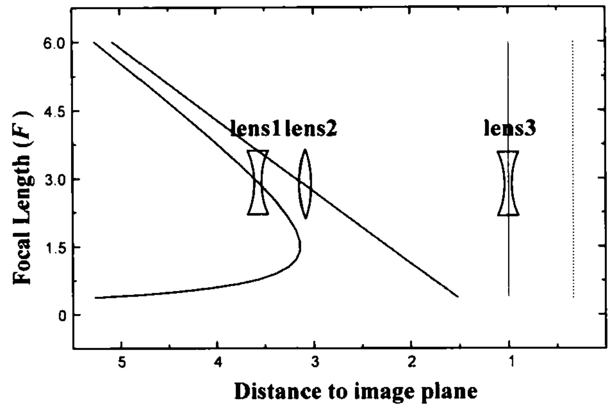

Figure 10. Loci of three-lens zoom system with $F_1 = -1$, $F_2 = 0{\cdot}95$, $F_3 = -2$, $M_3 = 1{\cdot}5$, $l_3' = 1$ and a zoom ratio of 16:1. This system has $d_1 = 0{\cdot}9$, $l_2' = 1{\cdot}9$ and $F_{12} = 1$ at the position where the system length is minimum during zooming.

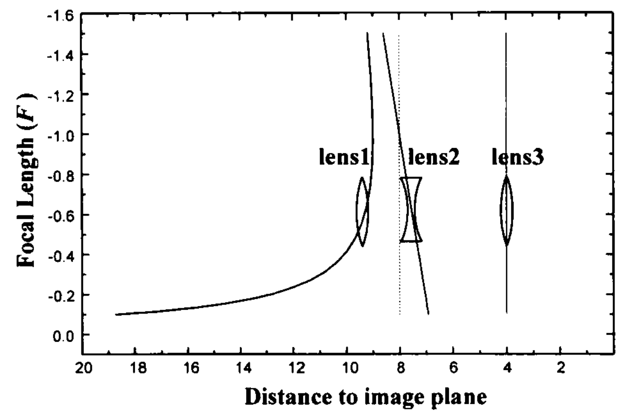

Figure 11. Loci of three-lens zoom system with $F_1 = 1$, $F_2 = -1{\cdot}2$, $F_3 = 2$, $M_3 = -1$, $l_3' = 4$ and a zoom ratio of 15:1. This system has $d_1 = 1$, $l_2' = 0$ and $F_{12} = 1$ at the position where the system length is minimum during zooming.

2.5.5. *Type V*

For segment 5 in figure 7, the range of F_{12} is from plus infinity to zero. Only the fifth solution area in table 1 belongs to this type. The vertex of hyperbolic curve is located on the positive transverse axis. By using the solution area (IVa) in figure 2 (*a*) and the range of l_2', we have $F_1 = 1$, $F_2 = -0{\cdot}4$, $F_4 = 0{\cdot}4$ and $M_3 = -1$. In this example, we choose the range of F_{12} from 10 to 0·1 with a zoom ratio of 100:1. The system has the minimum length with $d_1 = 1$, $l_2' = 0$ and $F_{12} = 1$. The zoom loci are shown in figure 12.

2.5.6. *Type VI*

For segment 6 in figure 7, the range of F_{12} is from minus infinity to $F_1F_2/(F_1 + F_2)$. Only the fourth solution area in table 2 with negative F_2 and F_{12} belongs to this type. The vertex of hyperbolic curve can be located in the third or fourth quadrant. Referring to the solution area (IV) in figure 2 (*b*) and the range

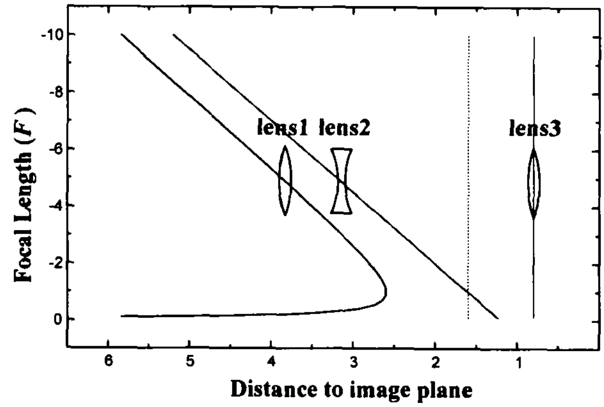

Figure 12. Loci of three-lens zoom system with $F_1 = 1$, $F_2 = -0{\cdot}4$, $F_3 = 0{\cdot}4$, $M_3 = -1$, $l_3' = 0{\cdot}8$ and a zoom ratio of 100:1. This system has $d_1 = 1$, $l_2' = 0$ and $F_{12} = 1$ at the position where the system length is minimum during zooming.

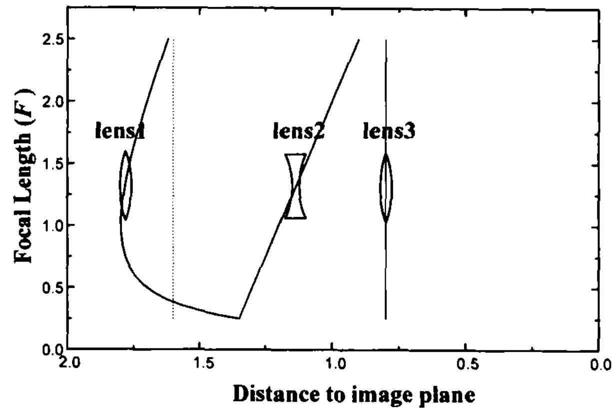

Figure 13. Loci of three-lens zoom system with $F_1 = 1$, $F_2 = -0{\cdot}2$, $F_3 = 0{\cdot}4$, $M_3 = -1$, $l_3' = 0{\cdot}8$ and a zoom ratio of 10:1. This system has $d_1 = 0{\cdot}6$, $l_2' = -0{\cdot}4$ and $F_{12} = -1$ at the position where the system length is minimum during zooming.

of l_2', we have $F_1 = 1$, $F_2 = -0{\cdot}2$, $F_3 = 0{\cdot}4$ and $M_3 = -1$. In this example, we choose the range of F_{12} from $-2{\cdot}5$ to $-0{\cdot}25$ with a zoom ratio of 10:1, We get $F_{12} = l_2' = -0{\cdot}25$ at $d_1 = 0$. The system has the minimum length with $d_1 = 0{\cdot}6$, $l_2' = -0{\cdot}4$ and $F_{12} = -1$. The zoom loci are shown in figure 13.

3. Conclusion

For designing a zoom system, the size of system and the slope of lens loci have been taken into account. From figures 8–13, we find that the lens locus of the middle lens is linear. This is due to the linear relationship between F_{12} and l_2' in equation (10). In some types, we may have an interlens separation of zero at one end of zooming. Usually, it is not useful to work in the neighbourhood of the end in a practical design. In this paper, we have not discussed the special condition in which $a_1 = 0$ $(F_1 + F_2 = 0)$. In this case, the solution is easily obtained by the same way as described in section 2. The centre of the hyperbola in equation (15) is located on the longitudinal axis in the d_1–l_2' coordinate graph.

In this paper, we have analysed the possible solutions areas in the focal length diagrams, the relation between d_1 and l_2', and the properties of lens loci during zooming. With the help of the solution range of l_2', the values of F_3 and M_3 are easily obtained to get a final real image and to keep d_2 positive in zooming. The analyses of six system types, corresponding to six segments in the d_1–l_2' coordinate graph, are very helpful for designers to select the positive and negative types of three lenses, to preview the shape of lens loci and to determine the ranges of F_{12}, d_1 and l_2'.

Acknowledgment

This project was supported by the National Science Council of the Republic of China under grant No. NSC-85-2215-E-009-004.

References

[1] Mann, A., and Thompson, B. J. (editors), 1993, *Selected Papers on Zoom Lenses*, SPIE Milestone Series, Vol. MS 85 (Bellingham, Washington: SPIE).
[2] Yeh, M. S., Shiue, S. G., and Lu, M. H., 1995, *Opt. Engng*, **34,** 1826.
[3] Yeh, M. S., Shiue, S. G., and Lu, M. H., 1996, *Opt. Engng*, **35,** 3348.
[4] Yeh, M. S., Shiue, S. G., and Lu, M. H., 1997, *Opt. Engng*, **36,** 1249.
[5] Oskotsky, M. L., 1992, *Opt. Engng*, **31,** 1093.